Received: 30 October 2021 | Revised: 26 September 2022 | Accepted: 7 November 2022

DOI: 10.4218/etrij.2021-0417

ORIGINAL ARTICLE

ETRI Journal WILEY

Factors affecting real-time evaluation of muscle function in smart rehab systems

Hyunwoo Joe[1] | Hyunsuk Kim[1] | Seung-Jun Lee[1] | Tae Sung Park[2] | Myung-Jun Shin[3] | Lee Hooman[4] | Daesub Yoon[1] | Woojin Kim[1]

[1]Mobility UX Research Section, Electronics and Telecommunications Research Institute, Daejeon, Republic of Korea

[2]Department of Convergence Medical Institute of Technology, Pusan National University Hospital, Busan, Republic of Korea

[3]Department of Rehabilitation Medicine, Pusan National University Hospital, Busan, Republic of Korea

[4]EXOSYSTEMS, Seoul, Republic of Korea

Correspondence
Woojin Kim, Mobility UX Research Section, Electronics and Telecommunications Research Institute, Daejeon, Republic of Korea.
Email: wjinkim@etri.re.kr

Funding information
This work was partly supported by Institute of Information & Communications Technology Planning & Evaluation (IITP) grant funded by the Korea Government (MSIT; No.2022-0-00501) and Korea Institute for the Advancement of Technology (KIAT) through the International Cooperative R&D program of the Ministry of Trade, Industry, and Energy (MOTIE; No. P0007114).

Abstract

Advancements in remote medical technologies and smart devices have led to expectations of contactless rehabilitation. Conventionally, rehabilitation requires clinicians to perform routine muscle function assessments with patients. However, assessment results are difficult to cross-reference owing to the lack of a gold standard. Thus, the application of remote smart rehabilitation systems is significantly hindered. This study analyzes the factors affecting the real-time evaluation of muscle function based on biometric sensor data so that we can provide a basis for a remote system. We acquired real clinical stroke patient data to identify the meaningful features associated with normal and abnormal musculature. We provide a system based on these emerging features that assesses muscle functionality in real time via streamed biometric signal data. A system view based on the amount of data, data processing speed, and feature proportions is provided to support the production of a rudimentary remote smart rehabilitation system.

KEYWORDS

biometric sensing, muscle function, real-time evaluation, rehabilitation, smart device

1 | INTRODUCTION

Stroke is the second leading cause of death worldwide, and the rate is not expected to subside [1–3]. Stroke survivors are required to perform rehabilitation exercises either by themselves or with the help of clinicians over long periods if they desire to recover the ability to lead independent lives. Notably, after the World Health Organization declared the COVID-19 outbreak a "pandemic" in February 2020, people's interest in remote rehabilitation services increased. The resulting remote technological boom has led to an impressive variety of long-distance collaboration, data collection, and physical manipulation capabilities [4]. Remote medical diagnoses and counseling capabilities are now a part of modern life. Even remote surgery has made vast improvements.

Presently, with rehabilitative therapy, stroke patients often need clinicians' direct intervention for assessment, physical support, and exercise. However, new biosensor-enabled applications and smart physical assisting devices have rendered the idea of remote stroke assessment and therapy a real possibility [5, 6].

Unfortunately, conventional in-person methods of muscle function assessment lack a systematic, comprehensive, and continuous gold standard, which makes it highly unlikely that a remote system of sensors and mechanical devices would be effectively fielded for a global community of patients.

Current popular tools include the Manual Muscle Testing (MMT) diagnostic method, the Fugl–Meyer Assessment (FMA), and the Brunnstrom Stages of Stroke Recovery, to name a few. Their scaled measures differ greatly, making it very difficult to port results from one method to another [7, 8]. Moreover, the prescribed physical treatments are inconsistent. Owing to these discrepancies, many experienced clinicians have developed their own interpretive or composite methods. Hence, to enable a remote smart rehabilitation capability, a rudimentary method-agnostic set of raw quantitative measures is needed that reflect the minute differences in muscle function based on real-time (RT) biometric signals. From this, a universal baseline capability can be developed from which clinicians can interface their favored diagnostic tools or even develop their own.

To these ends, we focus on the musculature of the upper limbs as proof of concept. After gaining Institutional Review Board approval from Pusan National University Hospital [9], we gathered real clinical stroke-patient data, divided the electromyography (EMG) signals into time and frequency domains, and compared abnormal and normal muscle functions. We then associated the results with the associated ground truth comprehensive medical decisions rather than analyzing each feature. From these comparisons and subsequent analyses, we propose a framework for RT biometric signal assessment and estimation. The technique is aimed at clinical decision support, but the output can easily be fed to simulators, functional electrical stimulation (FES), and robotic exoskeletons for remote therapy and movement support.

Our research contributions are as follows:

- A legitimate method-agnostic clinical decision-support capability that finally enables smart remote muscular function assessment and therapy options for stroke survivors.
- An RT data-inferencing function that enables instant biometric feedback using on-device sensors. Conventionally, an EMG signal resolution within 10 Hz is sufficient for estimating musculature movements [10]. Our system provides 50–100 times the required resolution, from 500 Hz to 1000 Hz.
- A minimum data throughput and processing standard to support the live streaming data requirement.
- A holistic pattern-based upper-body musculature function recognition capability that uses a moving-window sensory data measurement to provide movement prediction.

2 | BACKGROUND AND RELATED WORK

2.1 | Stroke and rehabilitation

Generally, stroke rehabilitation is divided into acute, subacute, recovery, and chronic stages, and most associated rehabilitation activities are performed in clinical settings. Gross motor functionality is normally handled by physical therapists, upper-limb fine motor function and cognition are handled by occupational therapists, and language capabilities are handled by language therapists. For gross motor area treatment, physical therapists adopt the proprioceptive neuromuscular facilitation (PNF) standard for nervous system therapy (e.g., electrotherapy) [11–13]. The rule of thumb is that 1 year is required from the onset of the stroke condition for maximum recovery. However, recent studies have shown that physical functionality continues to improve after 12 months [11]. Moreover, rehabilitation periods have been known to last from a few months to several years [11–13]. To achieve simultaneous physical and cognitive recovery, multidimensional biofeedback sensors are needed to collect and analyze complex musculature function data. Presently, "assist-as-needed" capabilities are employed to control a machinated exoskeleton to compensate for patient deficiencies during exercise, both at the clinic and elsewhere. However, this type of capability is not suitable for a combined user-centered smart remote assessment and self-rehabilitation services.

2.2 | Muscle function assessment

To support MMT, FMA, and Brunnstrom methods [12–14], EMG sensors and inertial measurement units (IMUs) are often used to measure isometric body movements [7, 8, 14, 15]. This convergence of techniques is promising, and maximum voluntary isometric contraction onset times and reference voluntary contraction thresholds have been advanced.

Most surface EMG signals are affected by sampling fraction and filtering, and interpretations differ depending on the object of analysis. Hence, the guidelines for different disease treatments are quite diverse. Note that IMU acceleration and angular velocity measures are multidimensional, assessments are largely subjective, and scales and window sizes are difficult to standardize [7, 8]. Therefore, a new baseline set of holistic measures is needed.

2.3 | Real-time muscle function measurement system

Clinicians evaluate EMG patterns to assess many types of bodily functions [16, 17], such as touch events [18] and hand and arm gestures [19]. The integration of EMG and IMU capabilities has enabled contactless RT estimation of patients' state of exercise and movement. Kim [20] conducted research that extracted EMG signals and desired patterns in real time, noting that the time for signal acquisition and pattern recognition should not exceed 300 ms [20, 21]. Moreover, a system of this design requires at least a 10-Hz frequency to adequately measure a person's movement. [10]. Notably, a higher frequency of measurement can enable instant feedback, which is vital for any conceived RT muscle function assessment system. Current portable contactless devices have limited resources and are unlikely to support RT feedback to clinicians. Therefore, their data must be off-loaded and transmitted periodically [22–24]. This process will not support a smart remote rehabilitation system.

3 | MUSCLE FUNCTION ASSESSMENT SCHEMES

3.1 | EMG signal analysis

EMG signals are acquired by attaching electrodes to the skin above a targeted muscle to detect its activity, such as contractions and relaxations. A raw EMG signal contains useful information as well as noise. Thus, meaningful features must be extracted from the signal before they can be used for muscle analysis [25]. EMG signals can be quantified in both time and frequency domains, and the analysis results often require one or the other for the best utility, such as determining muscle fatigue [26–29]. Table 1 lists the most common time and frequency domain measures.

The integrated EMG (IEMG) is the sum of absolute values of EMG signal amplitudes. IEMG is described with (1):

$$\mathrm{IEMG} = \sum\nolimits_{n=1}^{N} |x_n|, \tag{1}$$

where x_n represents the EMG signal in a window and N denotes the length of the EMG signal.

The mean absolute value (MAV) is the average of absolute values of EMG signal amplitudes in a window expressed as (2):

$$\mathrm{MAV} = \frac{1}{N}\sum\nolimits_{n=1}^{N} |x_n|, \tag{2}$$

where x_n represents the EMG signal in a window and N denotes the length of the EMG signal.

Mean value slope (MAVS) shows the differences in MAVs between adjacent windows. It is expressed as (3):

$$\mathrm{MAVS}_i = \mathrm{MAV}_{i+1} - \mathrm{MAV}_i;\ i = 1, \ldots, I-1, \tag{3}$$

where i is the number of EMG signal windows.

The simple square integral (SSI) is the integrated value of a simple square of EMG signal amplitudes in a window. It is expressed as (4):

$$\mathrm{SSI} = \sum\nolimits_{n=1}^{N} |x_n|^2, \tag{4}$$

TABLE 1 EMG time and frequency domain features for muscle function evaluation.

Features	Description
Type: TIME	
Maximum peak (positive, negative, dual)	Maximum value of the peak within a sliding window
Positive peak-interval (PP-I) mean	Average of peak intervals within a window
PP-I standard deviation (SD)	SD of the peak spacing within a window
Integrated EMG (IEMG)	Sum of absolute values within a window
Mean absolute value (MAV)	Average of absolute values within a window
MAV slope (MAVS)	MAV difference from previous windows
Simple square integral (SSI)	Sum of squared values (energy)
Variance (VAR)	Dispersion (power)
Root mean square (RMS)	Square root of the mean of squares
Type: FRQ	
Total power (TP)	Total sum of the frequency spectrum
Median frequency (MDF)	Center frequency at which the frequency spectrum is divided in half
Mean frequency (MNF)	Average of frequencies

where x_n represents the EMG signal in a window and N denotes the length of the EMG signal.

Variance (VAR) reflects the variance of EMG signal amplitudes. The average value of EMG signals is close to zero and is expressed as (5):

$$\mathrm{VAR} = \frac{1}{N-1}\sum_{n=1}^{N} x_n^2, \tag{5}$$

where x_n represents the EMG signal in a window and N denotes the length of the EMG signal.

The root mean square (RMS) is the value calculated by squaring EMG signal amplitudes, averaging their values, and calculating the results' square root. It is expressed as (6):

$$\mathrm{RMS} = \sqrt{\frac{1}{N}\sum_{n=1}^{N} x_n^2}, \tag{6}$$

where x_n represents the EMG signal in a window and N denotes the length of the EMG signal.

In this study, the fast Fourier transform (FFT) [26] was used to convert a signal from the time domain into the frequency domain; it is the most widely used method for doing this for EMG signals.

Total power (TP) is an aggregation of the EMG power spectrum. It is expressed as (7):

$$\mathrm{TP} = \sum_{i=1}^{M} P_i, \tag{7}$$

where P_i is the EMG power spectrum at frequency bin i and M is the length of the bin.

The median frequency (MDF) is the center frequency dividing the spectrum in half. It is expressed as (8) [24]:

$$\mathrm{MDF} = \frac{1}{2}\sum_{i=1}^{M} P_i, \tag{8}$$

where P_i is the EMG power spectrum at frequency bin i and M is the length of the bin.

The mean frequency (MNF) is the average of a set of frequencies calculated by summing its multiplied values with its spectrum powers and dividing the summed value by the sum of spectrum power. It is expressed as (9) [24]:

$$\mathrm{MNF} = \sum_{i=1}^{M} f_i P_i \Big/ \sum_{i=1}^{M} P_i, \tag{9}$$

where f_i is the frequency of EMG power spectrum at frequency bin i, P_i is the EMG power spectrum at frequency bin i, and M is the length of the bin.

Individual features that are acquired by the above methods can be useful in certain situations. However, not all features are useful for assessing the state of a patient's muscle function. Therefore, we adopted actual stroke patient data features distinguishable by time and frequency domains and found the most variables for muscle function assessment. The results are given in the experiment assessment section.

3.2 | IMU signal analysis

Table 2 lists candidate features that can be acquired from IMU data to assess muscle function. Please note that exploring the relationship between IMU-related features and muscle function is not within the scope of this investigation.

TABLE 2 IMU muscle function features.

Features	Description
Type: Origin	
Range of movement (ROM)	Maximum joint angle
Velocity	Joint movement speed
Acceleration	Joint motion acceleration
Steady-state error	Residual deviation (when joint angle is fixed)
Duration (delay)	Time taken to perform the target action (delay)
Type: Extraction	
Smoothness	Smoothness of movement (jerk)
Similarity of trajectory	Similarity to the normal trajectory
Stability	Compensatory movement
Type: EMG	
Onset time	Moment of muscle contraction from starting point
Type: EMG + IMU	
Reactive time	Moment of movement from muscle contraction
Efficiency	Movement performance efficiency compared to contraction power
Controllability	Motion–muscle coherence
Sustainability	Muscle contraction persistence

4 | PROPOSED REAL-TIME MUSCLE FUNCTION ASSESSMENT SYSTEM

The architecture of our proposed RT muscle function assessment system is shown in Figure 1. It consists of control software (SW) for managing sensors and processing and analyzing data. An interactive SW is used to analyze RT muscle functions using a library or application programming interface to access cognitive process algorithms based on the musculoskeletal model. The configuration includes synchronization technology for patient data supporting RT estimation. The system provides an external interface for acquiring biometric signals with accompanying cognitive computing hardware.

As shown in Figure 2, soft RT system operations are supported with an RT-patch that can be extended using a prioritized scheduling scheme. The system uses central processing unit (CPU) shielding and prioritization (Electronics and Telecommunications Research Institute [30–32]) to prevent multicore cache pollution and interruptions, and to prevent threads from interfering with each other. The computing module consists of a multiple thread model for sensor control orders for biodata processing and analysis. The module synchronizes and processes multisensor data while running algorithms to estimate muscle functions. The module enables emergency stop functions, depending on the state of a patient. Thus, a limited form of preemptive scheduling is adopted for fault tolerance. A producer–consumer data queue model prevents data process delays, and an RT manager enables on-device cognitive computing. The system supports TensorFlow Lite or custom neural-network libraries. In stable clinical experiments with stroke patients, this option was temporarily unselected. If a hardware accelerator is adopted, a device driver that supports the accelerator should be added. The memory manager manages sensing and feedback data for determining muscle states and levels, and it can manage previously learned patient data for inferring RT state changes.

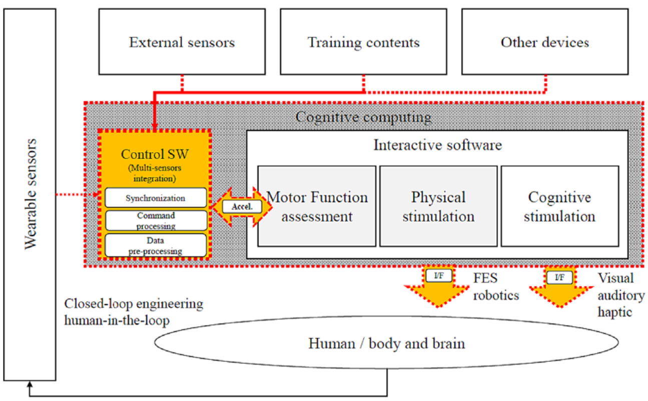

FIGURE 1 Proposed smart remote rehabilitation system architecture. FES, functional electrical stimulation; SW, control software; I/F (interface).

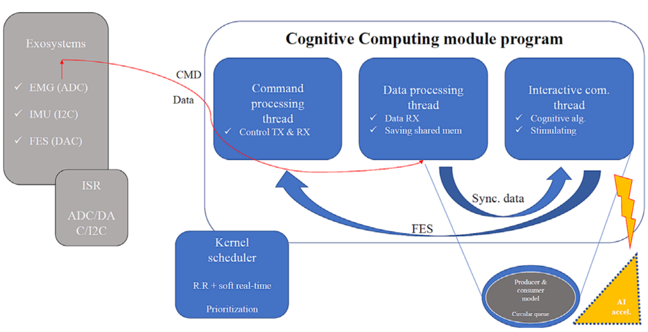

FIGURE 2 System software components with real-time options. EMG, electromyography; ADC, analog-to-digital conversion; I2C, inter-integrated circuit; IMU, inertial measurement unit; FES, functional electrical stimulation; DAC, digital-to-analog conversion; RR, round robin.

5 | EVALUATION

To evaluate our system, we investigated the known methodologies and factors affecting RT muscular function evaluation performance based on real clinical data. In this section, we describe the experimental environment and the method of assessment using real clinical data. We also examined paralysis vs. normal functionality differences and identified the best window and shift sizes to avoid interference while maximizing performance.

5.1 | Scenario for acquiring clinical data

This study was conducted at Pusan National University Hospital using data collected from one-on-one clinician–patient interactions. The subjects included 20 stroke-recovery patients who could adequately communicate with and follow the directions of medical staff. Figure 3 illustrates the EMG and IMU measurement system. Sensory data were generated from muscular movements using the FMA scale. EMG sensors were attached to the extensor carpi radialis, flexor carpi radialis, extensor digitorum communis, biceps brachii, triceps brachii, and anterior deltoid of participants. IMU sensors were attached to the wrist and back of the hand.

The system included an eight-channel EMG at 1 kHz, a two-channel IMU at 50 Hz, and an FES (Figure 3). Upon the order to initiate movement, participants raised their wrists as high as they could and maintained the

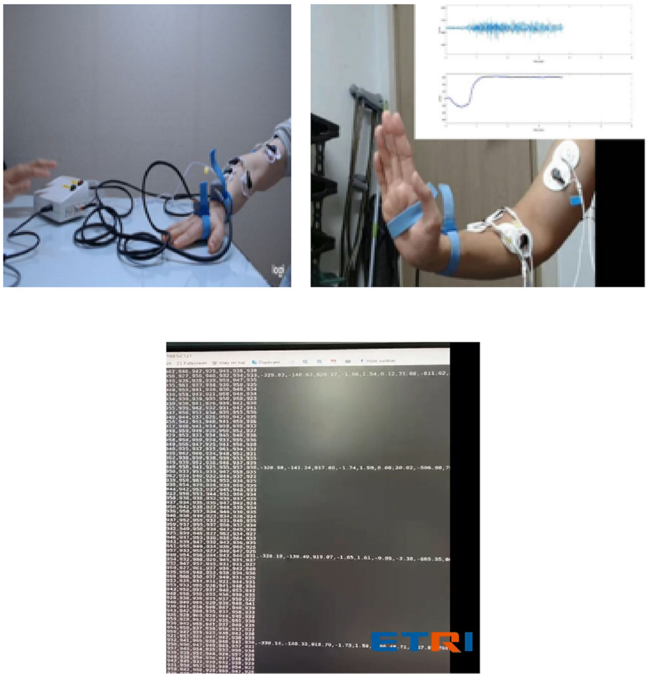

FIGURE 3 Biometric measurement system setup.

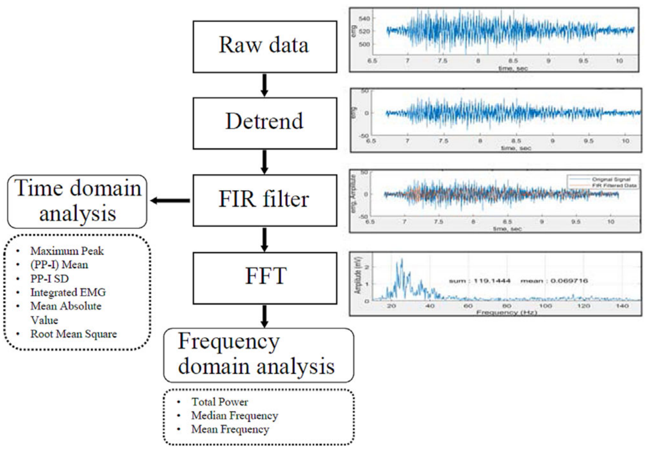

FIGURE 4 Electromyography signal processing flow. FIR, finite impulse response; FFT, Fourier transform; EMG, electromyography; PP-I, positive peak-interval.

posture for ∼5 s until they were ordered to stop. Then, they lowered their wrists to their original positions.

5.2 | Muscle function assessment

The process described in Figure 4 was carried out with a detrending process to eliminate noise. A Chebyshev finite impulse response low-pass filter was used to eliminate 200-Hz and below signals. FFT was carried out to convert time to frequency domain features.

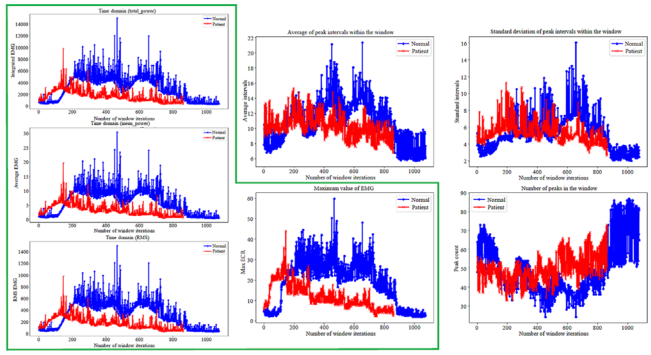

FIGURE 5 Time-domain feature differences between paralysis and normal muscle movements.

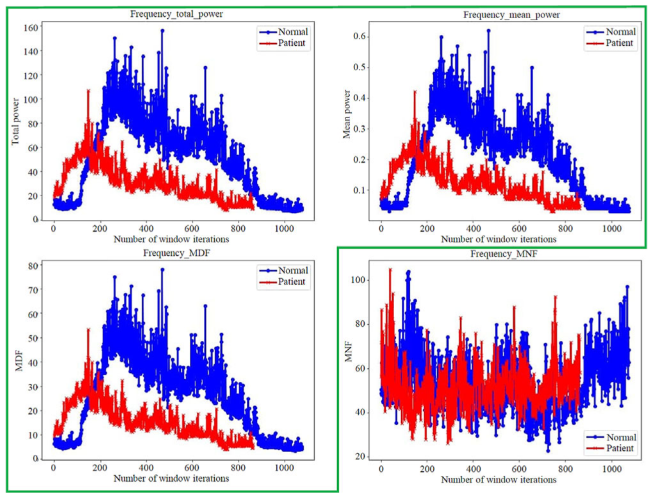

FIGURE 6 Frequency-domain feature differences between paralysis and normal muscle movements.

Figure 5 presents the analysis results of time-domain features. EMG power, maximum entropy power, RMS, and maximum value (green box) show distinguishable differences between paralysis and normal muscle functions. The average peak interval, standard peak interval, and number of peaks provide key time-domain features for assessment. Figure 6 presents the results of frequency-domain features. Spectrum total power, spectrum mean power, and median frequency (MDF; Figure 6, green box) show distinguishable differences between the measured values.

5.3 | RT muscle function assessment

5.3.1 | Accuracy

A MATLAB simulation was performed to determine if the different features were sufficiently distinguishable when relying on RT streaming data performance based on changing the streaming data window and shift sizes.

Window gaps between 100 ms and 500 ms were adjusted at 100-ms intervals. Given a 1-kHz measurement threshold, the window size can be adjusted in 100–500 units. The time-shift sizes were set to 5, 10, 20, 30, 40, and 50, which reflect the frequency of data collection. Figure 7 shows the analysis results based on these differences. We investigated several time-domain features (i.e., `integrated_emg`, `mean_emg`, `rms_result`, `meanCycle`, `stdCycle`, `max_ECR`, and `no_pks`), and in Figure 7, the *y*-axis reflects the difference of absolute feature values, and the *x*-axis reflects the shift size. Even with different window sizes, when the shift size is small, the results of integrated EMG, RMS, and `meanCycle` show significant differences. Therefore, smaller shift sizes equate to more easily distinguished paralysis vs. normal muscle movements; a 500-ms window gap with a shift size of five provided the best configuration.

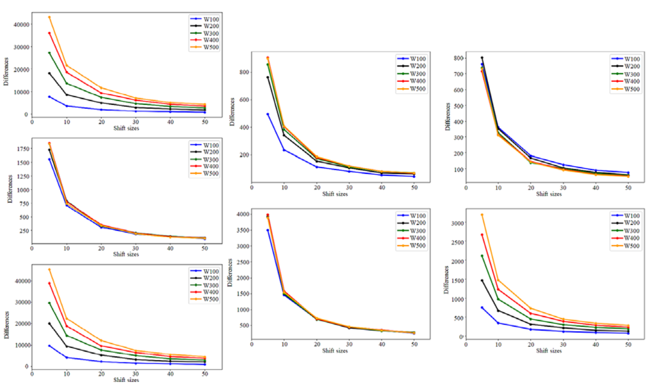

FIGURE 7 Time-domain feature utility based on changing window and time-shift values.

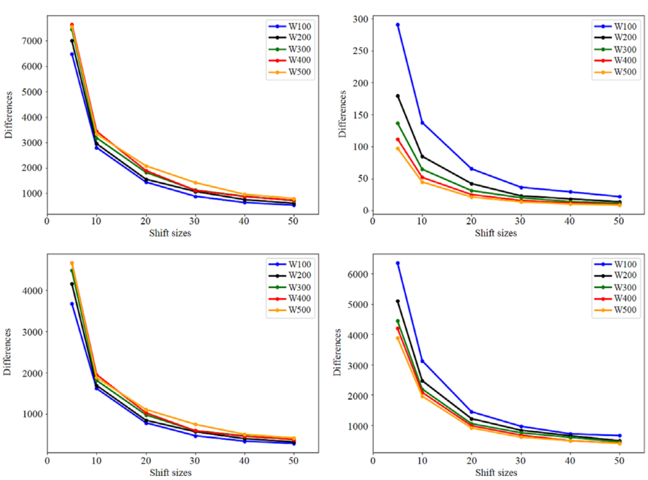

FIGURE 8 Frequency-domain feature utility based on changing window and time-shift values.

Figure 8 presents the differences in frequency domain data. Features of `tot_Fpower`, `mean_Fpower`, MDF, and MNF were analyzed. Again, the differences in total power and MDF were more apparent when the shifting size was small; a 500-ms window gap with a shift size of five provided the best configuration. The experiment showed that the accuracy of an RT muscle function assessment can be increased if the amount of relevant data is larger and the frequency is higher. Therefore, an algorithm that checks a vast amount of data frequently is needed.

5.3.2 | RT processing

Figure 9 displays the RT muscle function assessments using a Raspberry Pi system using Linux. External data were measured directly without library support. However, a TensorFlow Processing Unit (TPU) can be equipped for faster processing using TensorFlow Lite [33]. Two input/output services were provided: One for EMG, IMU, and FES, and the other for a robotics arm. Item $t1$ represents the moment of EMG/IMU data reception, and $t2$ represents the moment that FES/robotic arm commands are sent. RT processing time based on cognitive or pattern matching is expressed as $t2 - t1$, which excludes network delays from serial communications and Bluetooth. If a TPU is equipped, this duration should be reduced.

For all time- and feature-domain measures, the measurement cycle was 1 kHz, and all features were calculated in parallel. Related studies [22–24,34–39] focused on pattern recognition accuracy between movements and predictions. In contrast, we aimed to measure the difference between paralyzed and normal functions. Doing so can enable FES and exoskeletal support. The assist-as-needed mode of rehabilitation is likely the first area of improvement enabled by this research.

Unlike previous RT processing studies [34–39], we found optimal values by adjusting window and shift sizes

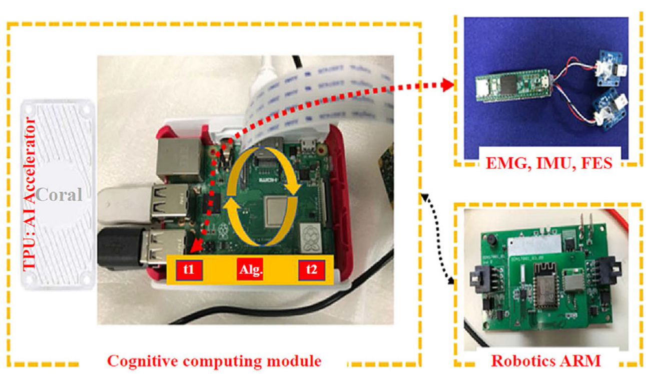

FIGURE 9 Real-time muscle function evaluation system.

TABLE 3 Real-time muscle function evaluation using the proposed system.

Shift					
Window	**5**	**10**	**20**	**25**	**50**
100	F	P	P	P	P
250	F	F	P	P	P
500	F	F	P	P	P
1000	F	F	F	P	P

Note: Sampling rate = 1 ms per sample; F = fail, P = pass.

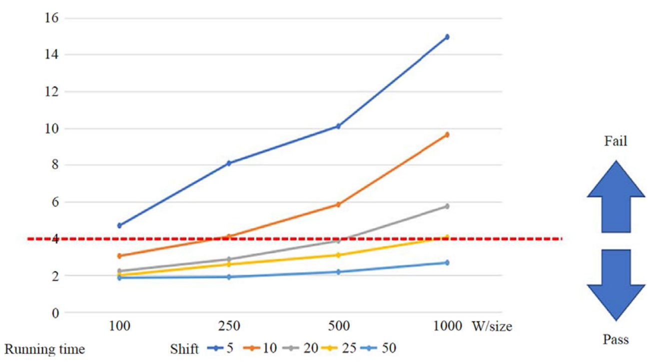

FIGURE 10 Real processing results based on shift and window sizes.

and considered the computer system capabilities related to each. In Table 3, "F" means "fail," "P" means "pass," and the number represents the number of samples. When the shift size was 25 or larger, even if the window size increased to 1000 ms, there was no data loss. However, when the shift size was five, even with a 100-ms window size, the RT system requirement was not met.

An additional experiment was conducted to further analyze the holistic results. All collected data were tested with different window and shift sizes, and processing times were measured. Figure 10 shows the results. The *y*-axis reflects performance time, and the *x*-axis represents window size. Given 4000 units of data, if the performance took longer than 4 s, the case was regarded as a failure. Consequently, the shift size was determined to be more important for RT muscle function assessment than the window size. Even as the window size grew, the RT requirement was met when the shift sizes were less than a measurable correlation factor.

Computing devices usually have hierarchical memory structures, except with simple board processors (e.g., Raspberry Pi), and their CPUs have pipeline structures. Notably, an RT computing system for our purposes must be capable of extracting, measuring, and differentiating time and frequency features. If a wide variety of calculation loops is needed in practical clinical settings, cache memory can become polluted, and pipeline processing penalties will increase. Even with an RT system patch, if the number of threads increases, the communication overhead will increase among threads. For RT assessment, the data structure and quantity handled by these threads should be extended. We confirmed that the desired approaches for developing an algorithm and establishing a system should focus on increasing accuracy by enlarging the window size rather than reducing the shift size.

Finally, we applied our method to the results of related works that used static window and shift sizes and analyzed the differences in hardware performance and processing times. Ma [22] fixed the window size to 512 and a shift size of 128. With our results, a shift size of 20 or more with a window of 500 was just as effective. Hence, the RT performance would be better with our method [22]. Furthermore, the accuracy of Ma's original 512 window size would be further improved with a 32 shift size. Alternatively, if the window size were to be set to 128, the RT requirement would be satisfied with a shift size of 10 or more.

6 | DISCUSSION AND FUTURE WORK

As shown in Figure 11, we extended our smart remote rehabilitation system to the assist-as-needed rehabilitation mode using smartly connected, collaborative intelligent sensors and actuators. This integration provides the following useful capabilities:

- Local and continuous long-term therapy (at-home rehabilitation)
- Market adaptability (versatility and scalability)
- Less involvement in doctor's supervision (intelligibility)
- Doctor visibility (compliance)

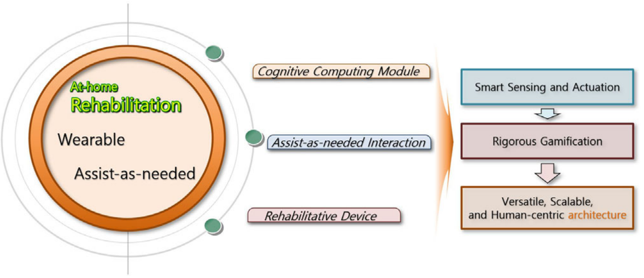

FIGURE 11 Smart remote rehabilitation vision.

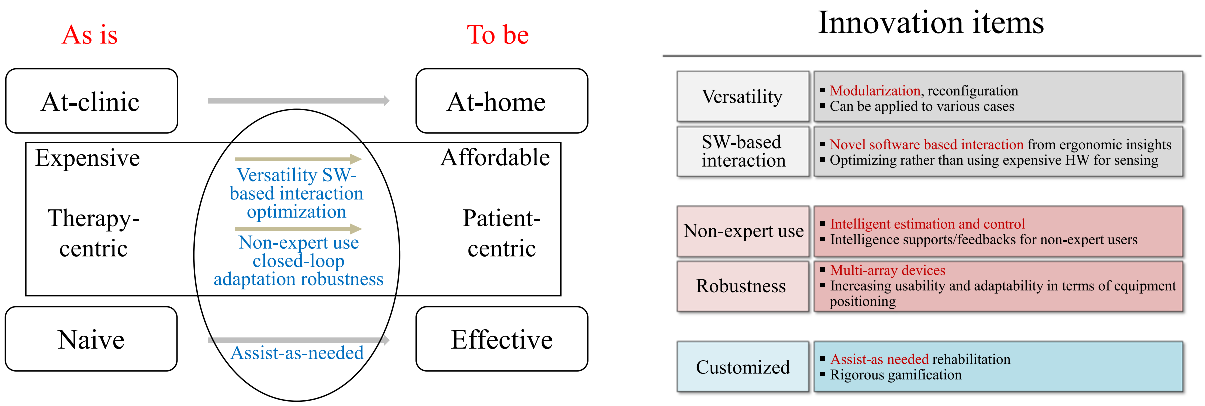

FIGURE 12 Innovation items for the smart remote rehabilitation system. SW, software; HW, hardware.

- Alignment with patient's needs and preferences (patient-centric)
- Effective performance (assist-as-needed)

Although several advanced rehabilitation systems and robotic devices have been adopted in clinical environments, support for remote rehabilitation is relatively scant, and fielded systems lack functionality, utility, and adaptability. On the other hand, demand is rapidly increasing. National and private health insurance companies are gradually expanding coverage to home medical equipment (HME). In terms of derivation technology, a neuromorphic module with smart connection, intelligent control, and EMG and FES management can be applied to other types of health monitoring and prevention. Moreover, new niche markets are expected to open. Nevertheless, the limitations faced by this study must be accounted for (Figure 12).

6.1 | Optimization of a real-time muscle function assessment and cognitive computing system

The COVID-19 pandemic hampered our study, restricting our access to both facilities and clinical data. Although the test population was relatively small, we clearly identified a variety of useful sensory features for assessing muscle function, and we identified some performance improvement opportunities (e.g., TPUs). To identify further optimization opportunities with applicable parametric information, a larger sample should be examined using our baseline capability. Doing so will also help refine the recommended window and shift sizes. In Figure 13, the left image shows a data capture screen, and the right image shows the processing time outputs.

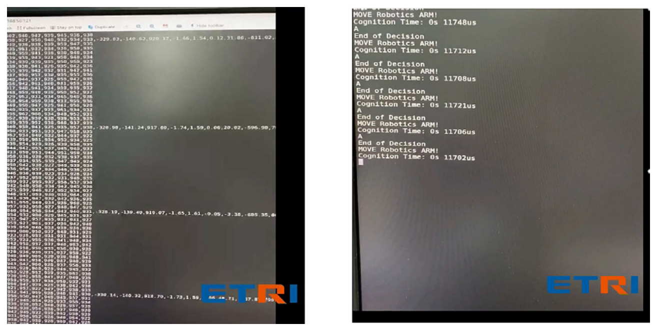

FIGURE 13 Cognitive computing test (left: capturing electromyography [EMG] and inertial measurement unit [IMU] data; right: controlling and stimulating a patient using the cognitive computing algorithm).

6.2 | Opportunities and limitations for contactless rehabilitation

Given that smart remote rehabilitation capabilities are a bona fide societal need, technologies based on EMG and IMU sensors will be essential to their production. Smart integrations with small-size, low-cost, and high-power smart devices will lead to great advancements in remote rehabilitation. However, we do not anticipate that there will ever be a completely autonomous system that will preclude human hands-on assistance. The best remote smart rehabilitation systems may still require friends or family members to assist with the therapeutic setup.

7 | CONCLUSION

This study proposed an RT muscle function assessment and decision-support system for remote smart rehabilitation. We acquired real clinical stroke patient data to identify meaningful features associated with normal and abnormal musculature. Furthermore, we provided a useful system view based on the amount of data, data processing speed, and feature proportions to support the production of a rudimentary remote smart rehabilitation system. We demonstrated its feasibility and identified system-related factors of accuracy in terms of muscle function assessment. We also examined paralysis vs. normal functionality differences and identified the best window and shift sizes to avoid interference while maximizing performance. These results will be useful as a reference for researchers and developers who will study and/or produce smart remote medical systems in the future. Future efforts should also consider available machine-learning algorithms.

ACKNOWLEDGMENTS

This work was partly supported by the Institute of Information & Communications Technology Planning & Evaluation (IITP) with a grant funded by the Korean Government (MSIT) (No. 2022-0-00501, Development of Wearable Device Assessment Technology, 50%) and the Korea Evaluation Institute of Industrial Technology (KEIT) with a grant funded by the Korean Government (MOTIE) (No. P0007114, InterConnected Intelligent Sensing and Actuation Solutions for At-home Rehabilitation (iCARE), 50%). The authors thank all iCARE project members in the Republic of Korea and Spain, as well as the patients who agreed to support our clinical trials (IRB No. 1870-012-068) in PNUH.

CONFLICT OF INTEREST STATEMENT

The authors declare that there are no conflicts of interest.

ORCID

Hyunwoo Joe https://orcid.org/0000-0002-7235-0830
Hyunsuk Kim https://orcid.org/0000-0003-4690-7049
Tae Sung Park https://orcid.org/0000-0001-6554-7638
Woojin Kim https://orcid.org/0000-0001-9589-784X

REFERENCES

1. World Health Organization, *Global health estimates summary tables: projection of deaths by cause, age and sex*, World Bank Income Group, Geneva, 2018.
2. J. K. Burton, E. E. Ferguson, A. J. Barugh, K. E. Walesby, A. M. Maclullich, S. D. Shenkin, and T. J. Quinn, *Predicting discharge to institutional long-term care after stroke: a systematic review and metaanalysis*, J. Am. Geriatr. Soc. **66** (2018), no. 1, 161–169.
3. A. David, R. Ramadoss, A. Ramachandran, and S. Sivapatham, *Activity recognition of stroke-affected people using wearable sensor*, ETRI J. 2023. https://doi.org/10.4218/etrij.2022-0242
4. C. Salgueiro, G. Urrùtia, and R. Cabanas-Valdés, *Available apps for stroke telerehabilitation during corona virus disease 2019 confinement in Spain*, Disabil. Rehabil. Assist. Technol. **12**, no. 2021, 1–11.
5. M. W. B. Zhang and R. Ho, *Harnessing the potential of the Kinect sensor for psychiatric rehabilitation for stroke survivors*, Technol. Health Care **24** (2016), no. 4, 599–602.
6. N.B. Oğur, M. Al-Hubaishi, and C. Çeken, *IoT data analytics architecture for smart healthcare using RFID and WSN*, ETRI J. **44** (2022) 1, 135–146.
7. T. S. Park, S. H. Kim, J. H. Kang, and M.-J. Shin, *The assessment of balance ability and development of indicators for normal adults in Korea in their 20s using digital equipment (FRA 510 S)*, J. Convergence Inform. Technol. **10** (2020), no. 9, 215–221.
8. S. H. An and C. S. Park, *The reliability and validity of short form of the Fugl-Meyer assessment scale in patients with stroke*, J. Special Education & Rehabil. Sci. **54** (2015), no. 1, 159–172.
9. Ethical approval, *Pusan National University Hospital Institutional Review Board* (IRB No. 1870-012-068).
10. H. Zeng and Y. Zhao, *Sensing movement: microsensors for body motion measurement*, Sensors **11** (2011), 638–660.
11. W. Kim, H. Joe, H. Kim, S.-J. Lee, D. Yoon, J. H. Jung, B. B. Acuña, H. Lee, J. F. Raton, C. F. Isoird, I. Mariñelarena, M. A. A. Alonso, M.-J. Shin and T. S. Park, *Requirements for upper-limb rehabilitation with FES and exoskeleton*, (International Conference on Intelligent Human Computer Interaction, Daegu, Republic of Korea), 2020, pp. 172–177.
12. J. Krukowska, M. Bugajski, M. Sienkiewicz, and J. Czernicki, *The influence of NDT-Bobath and PNF methods on the field support and total path length measure foot pressure (COP) in patients after stroke*, Neurol. Neurochir. Pol. **50** (2016), no. 6, 449–454.
13. J.-S. Wang, S.-B. Lee, and S.-H. Moon, *The immediate effect of PNF pattern on muscle tone and muscle stiffness in chronic stroke patient*, J. Phys. Ther. Sci. **28** (2016), no. 3, 967–970.
14. M. Bhadane, J. Liu, W. Z. Rymer, P. Zhou, and S. Li, *Re-evaluation of EMG-torque relation in chronic stroke using linear electrode array EMG recordings*, Sci. Rep. **6** (2016), no. 1, 1–10.
15. X. Song, S. Chen, J. Jia, and P. B. Shull, *Cellphone-based automated Fugl-Meyer assessment to evaluate upper extremity motor function after stroke*, IEEE Trans. Neural Syst. Rehabil. Eng. **27** (2019), no. 10, 2186–2195.
16. J. V. Basmajian and C. J. De Luca, *Muscles alive: their functions revealed by electromyography*, Williams & Wilkins, Baltimore, MD, 1985.
17. M. A. Oskoei and H. Hu, *Support vector machine-based classification scheme for myoelectric control applied to upper limb*, IEEE Trans. Biomed. Eng. **55** (2008), no. 8, 1956–1965.
18. H. J. Chizeck, O. Johnson, and J. Herron, *U.S. Patent No. 9,223,459*, U.S. Patent and Trademark Office, Washington, DC, 2015.
19. Korea Institute of Science and Technology, *Korea Patent No. 10-2014-0107741*, Korean Intellectual Property Office, 2014.
20. D.-H. Kim, C.-Y. Cho, and J. Ryu, *Real-time locomotion mode recognition employing correlation feature analysis using EMG pattern*, ETRI J. **36** (2014), no. 1, 99–105.
21. J.-U. Chu, I. Moom, Y.-J. Lee, S.-K. Kim, and M.-S. Mun, *A supervised feature-projection-based real-time EMG pattern*

recognition for multifunction myoelectric hand control, IEEE/ASME Trans. Mechatronics **12** (2007), no. 3, 282–290.
22. K. Ma, Y. Chen, X. Zhang, H. Zheng, S. Yu, S. Cai, and L. Xie, *sEMG-based trunk compensation detection in rehabilitation training*, Front. Neurosci. **13** (2019). https://doi.org/10.3389/fnins.2019.01250
23. Z. Yang and Y. Chen, *Surface EMG-based sketching recognition using two analysis windows and gene expression programming*, Front. Neurosci. **10** (2016). https://doi.org/10.3389/fnins.2016.00445
24. E. Trigili, L. Grazi, S. Crea, A. Accogli, J. Carpaneto, S. Micera, N. Vitiello, and A. Panarese, *Detection of movement onset using EMG signals for upper-limb exoskeletons in reaching tasks*, J. Neuroeng. Rehabil. **16** (2019), no. 1, 1–16.
25. A. Phinyomark, P. Phukpattaranont, and C. Limsakul, *The usefulness of wavelet transform to reduce noise in the SEMG signal*, In *EMG methods for evaluating muscle and nerve function*, Mark Schwartz, Rijeka, Croatia, InTech, 2012. https://doi.org/10.5772/25757
26. R. Boostani and M. H. Moradi, *Evaluation of the forearm EMG signal features for the control of a prosthetic hand*, Physiol. Meas. **24** (2003), 309–319.
27. A. Phinyomark, S. Hirunviriya, C. Limsakul, and P. Phukpattaranont, *Evaluation of EMG Feature Extraction for Hand Movement Recognition Based on Euclidean Distance and Standard Deviation*, (International Conference on Electrical Engineering/Electronics, Computer, Telecommunications and Information Technology, Chiang Mai, Thailand,) 2010.
28. F. Khanam and M. Ahmad, *Frequency Based EMG Power Spectrum Analysis of Salat Associated Muscle Contraction*, (International Conference on Electrical & Electronic Engineering, Rajshahi, Bangladesh), 2015. https://doi.org/10.1109/CEEE.2015.7428245
29. A. Phinyomark, S. Thongpanja, H. Hu, P. Phukpattaranont, and C. Limsakul, The Usefulness of Mean and Median Frequencies in Electromyography Analysis, in *Computational Intelligence in Electromyography Analysis—A Perspective on Current Applications and Future Challenges*, 2011. https://doi.org/10.5772/50639
30. H. Joe and H. Kim, *Effects of dynamic isolation for full virtualized RTOS and GPOS guests*, Future Gener. Comput. Syst. **70** (2017), 26–41.
31. R. Ma, F. Zhou, E. Zhu, and H. Guan, *Performance tuning towards a KVM-based embedded real-time virtualization system*, J. Inf. Sci. Eng. **29** (2013), 1021–1035.
32. J. Kiszka, *Towards Linux as a real-time hypervisor*, (Proceedings of the 11th Real-Time Linux Workshop), 2009, pp. 205–215.
33. Tensorflow lite. https://www.tensorflow.org/lite (accessed on 24.10.21)
34. X. Zhang, H. Huang, and Q. Yang, *Real-time implementation of a self-recovery EMG pattern recognition interface for artificial arms*, (Proceedings of the 2013 35th Annual International Conference of the IEEE Engineering in Medicine and Biology Society [EMBC], Osaka, Japan), 3–7 July 2013, pp. 5926–5929.
35. E. Mastinu, S. Member, and J. Ahlberg, *An alternative myoelectric pattern recognition approach for the control of hand prostheses: a case study of use in daily life by a dysmelia subject*, IEEE J. Transl. Eng. Health Med. **6** (2018), 1–12.
36. S. Raurale, J. McAllister, J. M. del Rincon, *EMG Wrsit-Hand Motion Recognition System for Real-Time Embedded Platform*, (IEEE International Conference on Acoustics, Speech and Signal Processing, Brighton, UK), 2019, pp. 1523–1527.
37. R. B. Woodward and L. J. Hargrove, *Adapting myoelectric control in real-time using a virtual environment*, J. Neuroeng. Rehabil. **16** (2019), 11.
38. T. A. Kuiken, B. A. Lock, R. D. Lipschutz, L. A. Miller, K. A. Stubblefield, and K. B. Englehart, *Targeted muscle reinnervation for real-time myoelectric control of multifunction artificial arms*, JAMA J. Am. Med. Assoc. **301** (2009), 619–628.
39. B. Chen, C. Chen, J. Hu, T. N. Nguyen, J. Qi, B. Yang, D. Chen, Y. Alshahrani, Y. Zhou, A. Tsai, and T. Frush, *A real-time myoelectric signal based fixed-bandwidth frequency-domain embedded system for robotic hand*, Front. Neurorobot. **16** (2022), 880073.

AUTHOR BIOGRAPHIES

Hyunwoo Joe received his BS, MS, and PhD degrees in computer science in 2005, 2007, and 2014, respectively, from Chungnam National University, Rep. of Korea. Since 2014, he has been with ETRI in Daejeon, Rep. of Korea. His research interests include embedded system software, system optimization, energy-aware intermittent computing, and resilient computing.

Hyunsuk Kim received her BS and MS degrees in computer science and engineering from Inha University, Rep. of Korea, in 1989 and 1992, respectively. She received a PhD in computer science and engineering from Chungnam National University Daejeon, Rep. of Korea in 2016. Since 1992, she has been a research member of ETRI, Daejeon, Rep. of Korea, and her research interests include human–vehicle interface, rehabilitation status assessment, mental state analysis, and data mining.

Seun-Jun Lee received his BS and MS degrees in electrical engineering from the Department of Electrical and Computer Engineering, Seoul National University, Seoul, Rep. of Korea, in 2009 and 2011, respectively. Since 2011, he has worked for ETRI in Daejeon, Rep. of Korea. His main research interests are human pose estimation and behavior recognition.

Tae Sung Park received his BS, MS, and PhD degrees in physical therapy from the Catholic University of Pusan, Busan, Rep. of Korea, in 2016, 2018, and 2022, respectively. Since 2017, he has worked at Pusan National University Hospital in

Busan, Rep. of Korea. Since 2022, he has been with the Department of Convergence at the Medical Institute of Technology, Pusan National University Hospital, Busan, where he is now a research professor. His main research interest is converged medical equipment.

Myung-Jun Shin received his BS and MS degrees in medicine from the Pusan National University School of Medicine, Busan, Rep. of Korea, in 2003 and 2009, respectively. He received his PhD degree in rehabilitation medicine from the Pusan National University School of Medicine, in 2014. Since 2007, he has worked for Pusan National University Hospital, Busan, Rep. of Korea and since 2019, he has been with the Department of Rehabilitation Medicine, Pusan National University Hospital where he is now an associate professor. His main research interest is converged medical equipment.

Hooman Lee received his BS degree in biosystem engineering from Seoul National University, Rep. of Korea in 2009 and MS degree in intelligence information convergence science from the same university in 2011. He was a researcher at the Intelligent Robotics Research Division, Department of Artificial Intelligence Research, at ETRI, Daejeon, Rep. of Korea, from 2011 to 2017. He currently runs EXOSYSTEMS Inc., Seoul, Rep. of Korea, a startup business. His main research areas include bio-signal analysis, digital biomarkers, digital health interventions, and compliant robot controls.

Daesub Yoon received his MS and PhD degrees in computer science and software engineering from Auburn University, Auburn, AL, USA. From 2001 to 2005, he was a research assistant with the Intelligent & Interactive System Laboratory at Auburn University. He joined ETRI, in Rep. of Korea, in 2005. His research interests include assistive technology, eye tracking, attentive user interfaces, mental workloads and human factors in rehabilitation, automated vehicles, and smart factories.

Woojin Kim received a BS degree in electrical engineering from the Korean Advanced Institute of Science and Technology, Daejeon, Rep. of Korea, and a PhD in mechanical and aerospace engineering from Seoul National University in Seoul, Rep. of Korea. In 2014, he joined ETRI, Daejeon, Rep. of Korea, where he is currently a senior researcher. His current research interests include human–robot interactions.

How to cite this article: H. Joe, H. Kim, S.-J. Lee, T. S. Park, M.-J. Shin, L. Hooman, D. Yoon, and W. Kim, *Factors affecting real-time evaluation of muscle function in smart rehab systems*, ETRI Journal **45** (2023), 603–614, DOI 10.4218/etrij.2021-0417.